Royal Norwegian Council
for Scientific and Industrial Research
(NTNF)

NORSAR

NORSAR Scientific Report No. 2-91/92

Semiannual Technical Summary

1 October 1991 – 31 March 1992

Kjeller, May 1992

7.8 Continuous seismic threshold monitoring of the northern Novaya Zemlya test site; long-term operational characteristics

Introduction

This paper is a summary of a comprehensive report (Kværna, 1992) giving a detailed analysis of the performance of the continuous threshold monitoring technique applied to the northern Novaya Zemlya test site for a full one-month period.

The theoretical background for and applications of the continuous seismic threshold monitoring metod (CSTM) have been described in several articles. The approach was introduced by Ringdal and Kværna (1989), who showed that by continuously monitoring the seismic amplitude level at several seismic stations or arrays, one can at any time obtain an instant network-based magnitude threshold for a given target region. The magnitude threshold can be interpreted as the maximum magnitude of a possible clandestine explosion, given a predefined level of confidence. In the context of a comprehensive or threshold test ban treaty, the continuous assessment of the magnitude thresholds makes it possible to focus attention upon those specific time intervals when realistic evasion opportunities exist, while retaining confidence that no treaty violation has occurred at other times.

Kværna and Ringdal (1990) presented results from a one-week experiment of continuously monitoring the northern Novaya Zemlya test site. Data from the Fennoscandian regional array network (ARCESS, FINESA, and NORESS), see Fig. 7.8.1, were used to calculate the magnitude thresholds. It was found that the test site could be consistently monitored at a very low magnitude level (typically $m_b = 2.5$). In fact, every occurrence of the threshold exceeding $m_b = 2.5$ could be explained as resulting from an identified interfering event signal either at teleseismic or regional distance.

The excellent capability of the Fennoscandian regional array network to monitor the northern Novaya Zemlya test site was further confirmed by an experiment where recordings of the Novaya Zemlya nuclear test of October 24, 1990 were downscaled to $m_b = 2.6$ and superimposed on different noise intervals (Kværna, 1991).

In the context of using CSTM as a tool in routine monitoring, it is important to determine how the method will work under different conditions. Variability in the seismic noise level, occurrences of large earthquakes and aftershock sequences, station downtimes and data quality problems are all factors that will influence the performance of CSTM. Again focusing on the northern Novaya Zemlya test site, using data from the Fennoscandian regional array network, we have analyzed one month of magnitude threshold data (February, 1992) for the purpose of evaluating the long-term operational characteristics of CSTM.

Analysis of network threshold peaks

Our monitoring experiment was conducted in the same way and with the same parameter settings as used by Kværna and Ringdal (1990). In Kværna (1992) the monitoring results

were presented in terms of plots covering one data day each. In Figs. A-1 to A-29 of the Appendix of that report, each covering one day of February, 1992, all time periods where the network magnitude thresholds at the 90% confidence level exceeded $m_b = 2.6$ have been identified.

For the remainder of this paper, the term magnitude threshold implies the magnitude threshold at the 90% confidence level.

From investigation of the distribution of all network CSTM data (totally 696 hours for February, 1992), we found that the network magnitude threshold exceeded $m_b = 2.6$ for about 50 minutes, see Fig. 7.8.2. This is only 0.12% of the total time, and we found $m_b = 2.6$ to be a suitable magnitude limit, in the sense that we were able to identify all interfering event signals causing the threshold to exceed this limit. One might of course argue that we should instead attempt to explain all peaks exceeding $m_b = 2.5$, but with reference to the actual CSTM data, we found that there were several intervals with m_b between 2.5 and 2.6, which we were not able to account for by signals from identified events. These intervals were all characterized either by a high background noise level at ARCESS, or with gaps in the ARCESS recordings.

Figs. 7.8.3 and 7.8.4 show two typical examples of a one-day plot (February 1 and 21). The upper three traces of each figure represent the magnitude thresholds obtained from the three indivitual arrays, whereas the bottom trace illustrates the network threshold. Typically, the individual array traces have a number of significant peaks for each 24-hour period, due to signals from interfering events (regional or teleseismic). On the network trace, the number and sizes of these peaks are significantly reduced, because an interfering event usually will not provide matching signals at all stations. From probabilistic considerations, it can in such cases be inferred that the actual network threshold is lower than these individual peaks might indicate.

The arrows on the one-day threshold plots indicate peaks with network magnitude threshold exceeding $m_b = 2.6$. A **T** at the arrow indicates that the peak is caused by signals from a teleseismic event, whereas an **R** indicates signals from a regional or local event. On three different occasions during February the threshold slightly exceeded 2.6 due to gap in the ARCESS recordings. These peaks were indicated by a **G** at the arrows.

A summary of the threshold peaks and the events causing the peaks is given in Table 7.8.1 covering the entire month of February 1992. Following the definition of the CSTM peaks (i.e., date, time, magnitude threshold, and number of seconds with the threshold exceeding $m_b = 2.6$), there is a bulletin of the events causing the peaks in the magnitude threshold traces. From Table 7.8.1 it can be seen that in some cases more than one event is contributing to the same peak in the threshold trace.

During the first half of February, there were several large teleseismic events causing increases in the network threshold (see events reported by the Quick Epicenter Determinations (QED) of the USGS), whereas during the second half of February, almost all CSTM peaks were caused by regional events. The regional events were all processed and located by the Intelligent Monitoring System (IMS) (Bache et al., 1990). The epicenters of the

regional events of Table 1 are plotted on the map of Fig. 7.8.5. Except for one felt earthquake in southern Norway (M_L = 3.26), the events are most likely mining explosions, as their epicenters coincide with known mining sites. Within the context of practical monitoring, it is interesting that for a 5-day period (February 23 through 27) there were no threshold peaks exceeding m_b = 2.6.

Continuous thresholds during noise conditions

For the purpose of analyzing the long-term fluctuations of the magnitude thresholds, we have for every 4-hour interval computed the median thresholds. The robust median estimator has been chosen to ensure that we are minimizing the influence of the short-term event peaks. These statistics have been computed for the network and for each array separately. The thresholds are all derived from filtered array beams, and thereby reflect the noise fluctuations within the applied frequency bands. The frequency filters used for ARCESS, FINESA and NORESS are 3.0-5.0 Hz, 2.0-4.0 Hz and 1.5-3.5 Hz, respectively.

Fig. 7.8.6a illustrates the results for each array for the month of February. It is clearly seen that ARCESS (the lower dashed line) has the best average capability for monitoring the northern Novaya Zemlya test site. Except for a few short time intevals, ARCESS has on the average lower magnitude thresholds than any of the other two arrays (NORESS - solid line, FINESA - upper dashed line). The ARCESS threshold curve has five pronounced peaks during the month, and shows internal variations of more than 0.5 m_b units. During quiet noise conditions, the median magnitude thresholds fluctuate around m_b = 2.0, but during the high-noise periods the thresholds approaches m_b = 2.5. Two of the peaks have been verified to correlate with severe wind and weather conditions in the ARCESS region, and it is also likely that the other three peaks are weather generated.

Compared to ARCESS, the NORESS magnitude thresholds show rather small variations, and fluctuate between m_b 2.4 and 2.5 during the entire period, see Fig. 7.8.6a. The small diurnal variations (of the order of 0.1 m_b units), are consistent with the findings of Fyen (1990). He found that for frequencies below 2 Hz, there was little difference between daytime and nighttime noise levels, whereas at higher frequencies, the diurnal variations are more significant (0.2-0.3 m_b units). It is only for a short time interval on February 6 that NORESS on the average has the best monitoring capability of the three arrays, but it has to be emphasized that this is not necessarily representative for time periods when seismic signals are present.

The median magnitude thresholds of FINESA, given by the top dashed line of Fig. 7.8.6a, exhibit strong weekly and diurnal variations. The diurnal variations are particularly significant on workdays. One peak for each of the five workdays are followed by a quiet weekend, reflecting the relative behavior of the background noise field in the frequency band of the P-beam steered towards Novaya Zemlya (2.0-4.0 Hz). The median thresholds during the weekends are approaching that of NORESS, whereas the workday levels are 0.2 to 0.4 m_b units higher. From Fig. 7.8.6a it can thus be inferred that FINESA on the average is contributing less than the other two arrays to the network monitoring capability of the northern Novaya Zemlya test site, but again, this may not be representative for time periods when seismic signals are present.

In Fig. 7.8.6b, we compare the median network performance (solid line) and the median ARCESS performance (dashed line) for monitoring the northern Novaya Zemlya test site. It is seen that when the ARCESS thresholds are low, the two curves almost coincide, implying that ARCESS alone determines the average network monitoring performance. However, during the ARCESS peak periods, the network curve is lower. This shows that even during background noise conditions, the other two arrays (FINESA and NORESS) contribute to lowering the magnitude thresholds.

We have in this section discussed the average properties of the CSTM performance of the Fennoscandian array network for monitoring the northern Novaya Zemlya test site. We have concluded that for most of the time, ARCESS is the array with the best capability, but that the other two arrays also play an important role, particularly when the ARCESS noise level is high.

Continuous thresholds during intervals with interfering signals

The dramatic improvement in the practical monitoring capability when using a network of arrays instead of a single array is illustrated in Fig. 7.8.7. We have for the month analyzed counted the number of threshold peaks exceeding a given magnitude, both for the network and for the best array (ARCESS). The barplots of Fig. 7.8.7 show that at a threshold of 2.6, the number of network threshold peaks are reduced by a factor of five in comparison to the threshold peaks at ARCESS alone (i.e., from 293 to 56). At a threshold of 3.0 the improvement is better than a factor of ten (i.e., from 41 to 3).

Conclusions

This work has documented the practical capability of the Continuous Seismic Threshold Monitoring method to monitor a specific nuclear test site at a very low threshold over an extended time period.

Specifically, we have used the Fennoscandian array network (NORESS, ARCESS and FINESA) to monitor the northern Novaya Zemlya test site for one full month (February 1992). We have shown that the magnitude threshold stays below $m_b = 2.50$, 99.72% of the total time. We have further "explained" all of the peaks exceeding $m_b = 2.6$ as resulting from one of the following three conditions: 1) a "large" identified teleseismic event, 2) a "large" identified regional event and 3) a short outage of the most important array (ARCESS).

The natural question is then as follows: Do these results imply that at the given confidence level there has been no seismic event of mb $\geq$ 2.6 at the test site during February 1992?

The answer is in practice "yes", since such an event only could have occurred during one of the time intervals when the network threshold trace exceeds 2.6. We have noted that the combined time span of such exceedances was only 50 minutes, or 0.12% of the total time. Since all the peaks were explained as resulting from known causes, it seems extremely unlikely that an event of mb 2.6 actually occurred during one of these short event intervals.

In theory, in a hypothetical monitoring situation for a comprehensive test ban treaty, there might be an "evasion" possibility if any of such high threshold periods could be predicted. But we do not consider this to be a realistic scenario. First, such predictions require exact knowledge of the configuration and the performance of the monitoring network, and second, there are a lot of practical problems involved in carrying out such a clandestine explosion so that the probability of getting detected is very high.

We have studied the relative contributions of the three arrays and found that ARCESS is clearly the most important, followed by NORESS and FINESA. During time periods when the ARCESS noise level is high, or when there are interfering events, the relative contributions of NORESS and FINESA increase significantly. The redundancy created by using several arrays is also essential during outages of one or more of the arrays.

The average magnitude thresholds at FINESA exhibit strong weekly and diurnal variations. The latter are particularly significant on workdays. The average NORESS thresholds show rather small variations, whereas at ARCESS, internal differences of more than 0.5 m_b units are observed. The peak periods at ARCESS are most likely caused by severe wind and weather conditions.

In the near future, additional array stations are planned for installation in the Arctic region. These stations would contribute to further improving the CSTM capability, both for Novaya Zemlya and on a general regional basis. This will be the subject for additional studies in the future.

T. Kværna

References

Bache, T., S. R. Bratt, J. Wang, R.M. Fung, C. Kobryn and J. W. Given (1990), The Intelligent Monitoring System, *Bull. Seism. Soc. Am.*, 80, Part B, 1833-1851.

Fyen, J. (1990): Diurnal and seasonal variations in the microseismic noise level observed at the NORESS array, *Phys. Earth Planet. Inter.*, 63, 252-268.

Kværna, T. (1992): Continuous seismic threshold monitoring of the northern Novaya Zemlya test site; long-term operational characteristics, AFGL Sci. Rep. No. 12, NORSAR, Kjeller.

Kværna, T. and F. Ringdal (1990): Continuous threshold monitoring of the Novaya Zemlya test site, *Semiannual Tech. Summary, 1 Apr - 30 Sep 1990*, NORSAR Sci. Rep. 1-90/91, NORSAR, Kjeller, Norway.

Kværna, T (1991): Threshold monitoring of Novaya Zemlya: A scaling experiment, *Semiannual Tech. Summary, 1 Oct 1990 - 31 Mar 1991*, NORSAR Sci. Rep. 2-90/91, NORSAR, Kjeller, Norway.

Ringdal, F. and T. Kværna (1989): A multi-channel processing approach to real-time network detection, phase association, and threshold monitoring, *Bull. Seism. Soc. Am.*, 79, 1927-1940.

Date	TM peak	Mag	Sec	Ev	Or. time	Lat	Lon	Dep	Mag	Bull	Region
02/01	11.46.11	2.66	20	R	11.46.08.8	67.592	30.300	0F	2.46	IMS	European Russia
02/01	19.12.08	2.99	88	T	19.04.05.3	35.164	139.702	107	5.6	QED	S.coast of Honshu
02/02	05.04.20	2.63	12	R	05.05.01.4	67.659	33.417	0F	2.41	IMS	European Russia
02/02	17.51.03	2.65	9	T	05.05.01.4	67.659	33.417	33F	5.5	QED	Kuril Islands
02/03	13.55.17	2.69	15	R	13.54.44.6	60.836	29.220	0F	2.41	IMS	European Russia
02/05	05.40.43	2.72	15	T	05.33.11.4	45.021	150.972	33F	5.6	QED	Kuril Islands
02/05	10.56.54	2.64	2	T	10.54.38.0	44.600	150.500	33F	4.3	NORSAR	Kuril Islands
02/05	13.21.09	2.90	69	T	13.13.42.5	52.163	-170.130	48	5.4	QED	Fox Islands
02/05	23.14.43	2.65	8	T	23.10.50.9	31.407	66.825	33F	5.1	QED	Afghanistan
02/06	01.23.52	2.95	181	T	01.12.41.2	-5.609	103.271	55	6.0	QED	Southern Sumatra
02/06	03.42.24	2.71	77	T	03.35.17.2	29.511	95.635	33F	5.6	QED	Xijang-India border
02/06	04.05.32	2.63	4	T	03.54.43.7	-5.374	103.197	72	5.5	QED	Southern Sumatra
02/06	05.13.26	2.63	3	T	04.57.28.0	-33.400	-175.200	33F	3.8	NORSAR	Kermadec Islands
02/06	09.19.03	2.78	39	R	09.18.47.9	61.243	29.875	0F	2.07	IMS	Finland-Russia border
				R	09.19.55.1	68.147	32.846	0F	1.90	IMS	European Russia
02/06	12.19.03	2.61	3	R	12.21.00.0	69.344	30.570	0F	2.14	IMS	Norway-Russia border
02/06	16.27.43	2.66	9	R	16.28.20.4	67.176	20.792	0F	1.83	IMS	Sweden
02/07	00.13.59	2.88	49	T	00.06.28.6	43.140	146.611	54	5.4	QED	Kuril Islands
02/07	06.42.13	2.67	20	T	06.35.26.0	52.925	159.555	49	5.3	QED	Off east coast of Kamchatka
02/07	08.38.36	2.66	15	R	08.41.05.1	67.633	33.715	0F	2.41	IMS	European Russia
02/07	09.20.39	2.61	1	R	09.21.16.4	68.190	32.875	0F	1.98	IMS	European Russia
				R	09.23.00.4	67.969	32.870	0F	1.92	IMS	European Russia
				R	09.25.08.3	59.298	26.399	0F	1.06	IMS	European Russia
02/07	09.54.59	2.65	15	T	09.48.38.7	55.795	160.753	138	5.0	QED	Kamchatka
02/07	09.59.36	2.64	5	R	10.00.44.9	64.692	30.728	0F	2.11	IMS	Finland-Russia border
02/07	12.18.59	2.80	21	R	12.20.52.2	69.329	30.842	0F	2.40	IMS	Norway-Russia border
02/08	11.44.28	2.69	29	R	11.44.41.2	67.648	30.594	0F	2.24	IMS	European Russia
02/09	04.09.14	2.63	5	R	04.09.41.1	67.574	33.741	0F	2.35	IMS	European Russia
02/09	07.56.42	2.57	-	T	07.49.21.5	51.497	-178.364	66	5.1	QED	Andreanof Islands
02/09	22.08.59	2.84	47	T	22.01.58.4	47.982	152.979	123	5.6	QED	Kuril Islands
02/12	01.09.22	2.82	42	T	01.02.01.9	51.299	177.926	33F	5.2	QED	Rat Islands
02/13	01.45.47	2.77	70	T	01.29.17.1	-15.923	166.215	33F	6.1	QED	Vanuatu Islands
02/13	02.45.31	2.82	54	T	02.38.18.4	53.576	-165.706	44	5.5	QED	Fox Islands
02/13	23.34.08	2.72	33	R	23.35.20.5	67.720	21.067	0F	1.84	IMS	Sweden
02/14	08.23.25	2.99	136	T	08.18.27.7	53.576	-165.706	33F	5.3	QED	Lake Baykal Region
02/14	08.48.02	2.61	1	R	08.48.20.2	67.391	32.939	0F	2.31	IMS	European Russia
02/14	12.19.23	2.96	115	R	12.21.00.9	69.322	30.727	0F	2.50	IMS	Norway-Russia border
02/15	11.47.38	2.62	1	R	11.49.21.2	67.656	30.374	0F	1.87	IMS	European Russia
02/15	12.57.21	2.76	61	T	12.52.55.0	42.846	46.588	33F	4.7	QED	Eastern Caucasus
02/16	08.49.11	2.70	27	R	08.49.50.5	67.636	33.547	0F	2.54	IMS	European Russia
02/16	21.55.47	2.53	-	R	21.54.36.6	67.667	20.841	0F	1.03	IMS	Sweden
02/17	00.04.52	3.13	136	T	00.01.56.7	79.190	124.625	10	5.8	QED	East of Severnaya Zemlya
02/17	08.13.48	2.65	27	G							Gap in ARCESS recording
02/17	14.23.57	2.71	33	R	14.25.24.0	69.638	30.430	0F	1.95	IMS	Norway-Russia border
02/17	15.45.13	2.63	4	G							Gap in ARCESS recording
02/18	12.42.04	2.68	8	R	12.42.01.9	59.337	27.065	0F	2.61	IMS	European Russia
02/19	06.40.25	2.91	226	R	06.39.32.9	59.240	10.886	0F	3.26	IMS	Southern Norway
02/19	12.26.49	3.25	302	R	12.25.03.0	69.257	30.575	0F	2.09	IMS	Norway-Russia border
				R	12.26.30.0	64.722	30.553	0F	2.78	IMS	Finland-Russia border
02/19	12.42.45	2.88	33	R	12.43.59.4	67.595	33.647	0F	2.46	IMS	European Russia
02/20	20.52.21	2.55	-	T	20.35.24.3	-33.498	-179.673	48	5.9	QED	South of Kermadec Islands
02/20	21.16.05	2.79	60	R	21.16.27.7	67.647	33.555	0F	1.98	IMS	European Russia
				R	21.16.50.5	67.918	33.951	0F	2.39	IMS	European Russia
02/21	08.59.39	2.74	103	R	08.59.25.1	67.657	33.791	0F	2.63	IMS	European Russia
02/21	11.01.46	3.14	173	R	11.01.53.5	64.672	30.801	0F	2.72	IMS	Finland-Russia border
02/21	12.49.06	2.99	135	R	12.50.11.2	69.341	30.688	0F	2.16	IMS	Norway-Russia border
				R	12.51.02.8	69.380	30.683	0F	2.46	IMS	Norway-Russia border
02/21	16.32.43	2.80	42	R	16.32.43.4	67.117	21.049	0F	2.02	IMS	Sweden
02/22	11.45.00	2.72	44	R	11.46.12.7	67.485	29.529	0F	1.87	IMS	Finland-Russia border
				R	11.46.59.0	67.558	30.328	0F	2.24	IMS	European Russia
02/22	11.59.31	2.70	35	R	12.00.18.7	67.599	33.659	0F	2.50	IMS	European Russia
02/28	08.58.22	2.75	36	R	08.58.59.1	67.617	33.769	0F	2.50	IMS	European Russia
02/28	12.07.37	2.63	2	R	12.09.56.9	59.170	27.332	0F	1.80	IMS	European Russia
02/28	12.19.10	2.69	37	G							Gap in ARCESS recording
02/28	12.43.14	2.92	243	R	12.45.11.0	69.365	30.647	0F	2.52	IMS	Norway-Russia border
02/28	14.30.16	2.68	17	R	14.30.29.5	67.709	33.695	0F	2.16	IMS	European Russia
				R	14.31.39.7	67.522	33.677	0F	2.31	IMS	European Russia

Table 7.8.1. List of peaks in the network threshold traces and the events causing the peaks. Following the definition of the CSTM peaks (i.e., date, time, maximum magnitude threshold, and number of seconds with the threshold exceeding $m_b = 2.6$), there is a bulletin of the events causing the peaks in the magnitude threshold traces. It can be seen that in some cases more than one event is contributing to the same peak in the threshold trace.

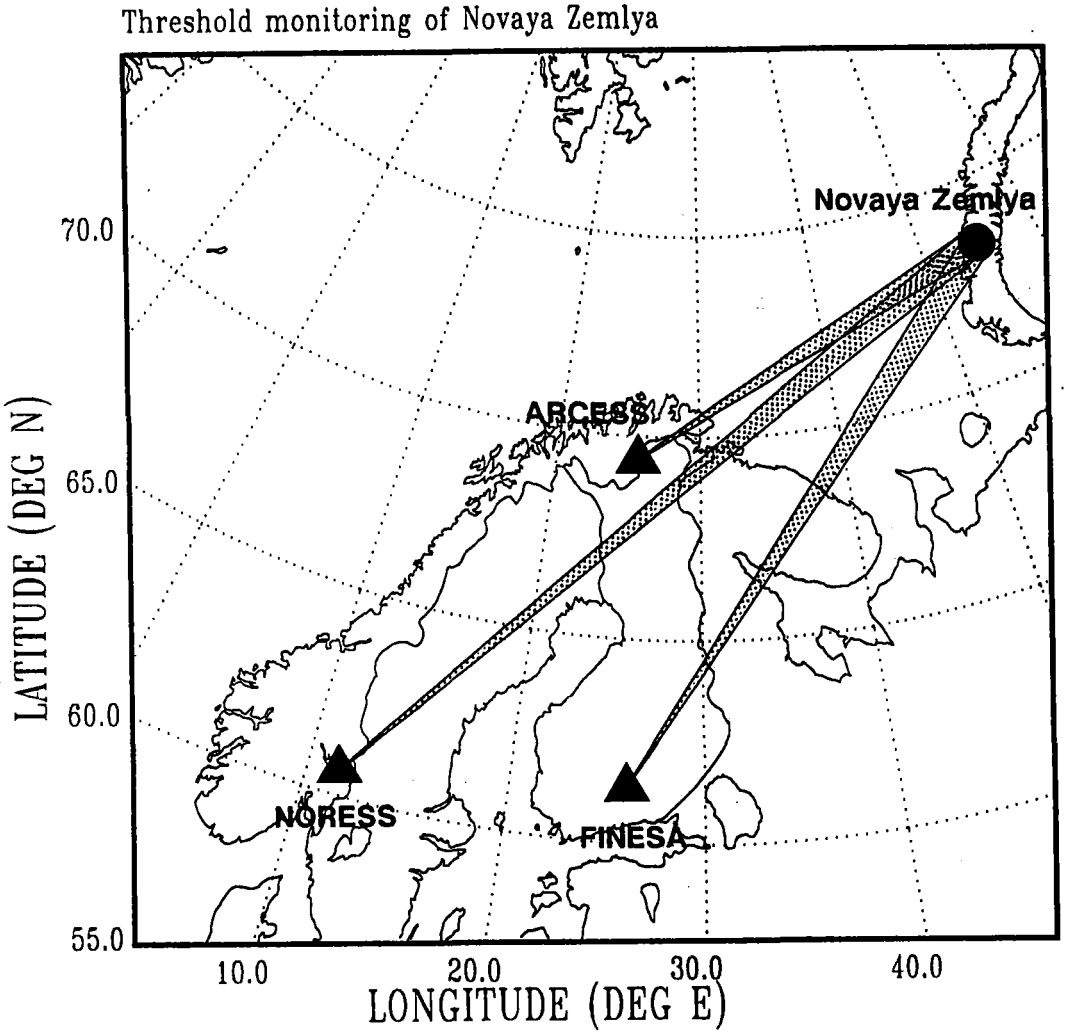

Fig. 7.8.1. Map showing the location of the northern Novaya Zemlya test site and the Fennoscandian array network. The distances of the three arrays from the test site are for NORESS 2280 km, for ARCESS 1100 km and for FINESA 1780 km.

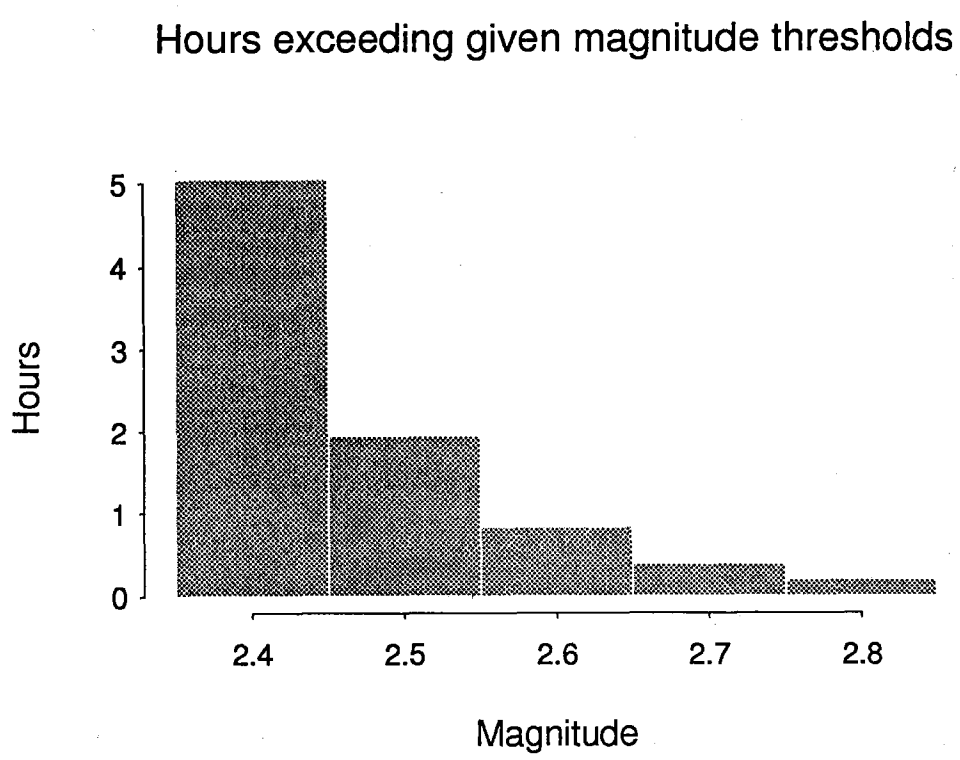

Fig. 7.8.2. Barplot showing the number of hours where the 90% network magnitude threshold exceeds a given magnitude, for the month of February, 1992.

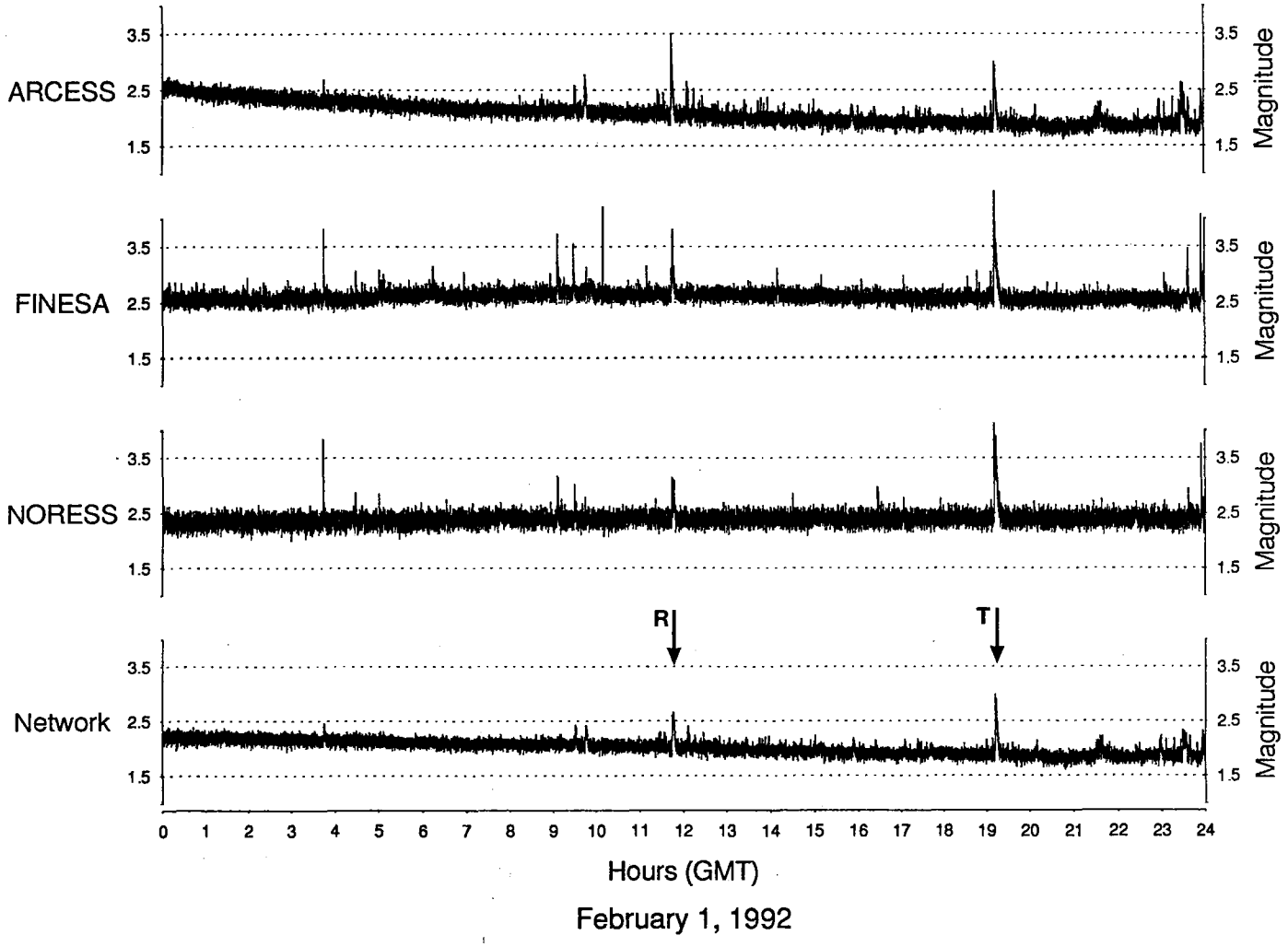

Fig. 7.8.3. The upper three traces represent the 90% magnitude thresholds obtained from the individual arrays, whereas the bottom trace illustrates the network threshold. The arrows indicate peaks with network magnitude threshold exceeding $m_b = 2.6$. A **T** at the arrow indicates that the peak is caused by signals from a teleseismic event, whereas an **R** indicates signals from a local or regional event.

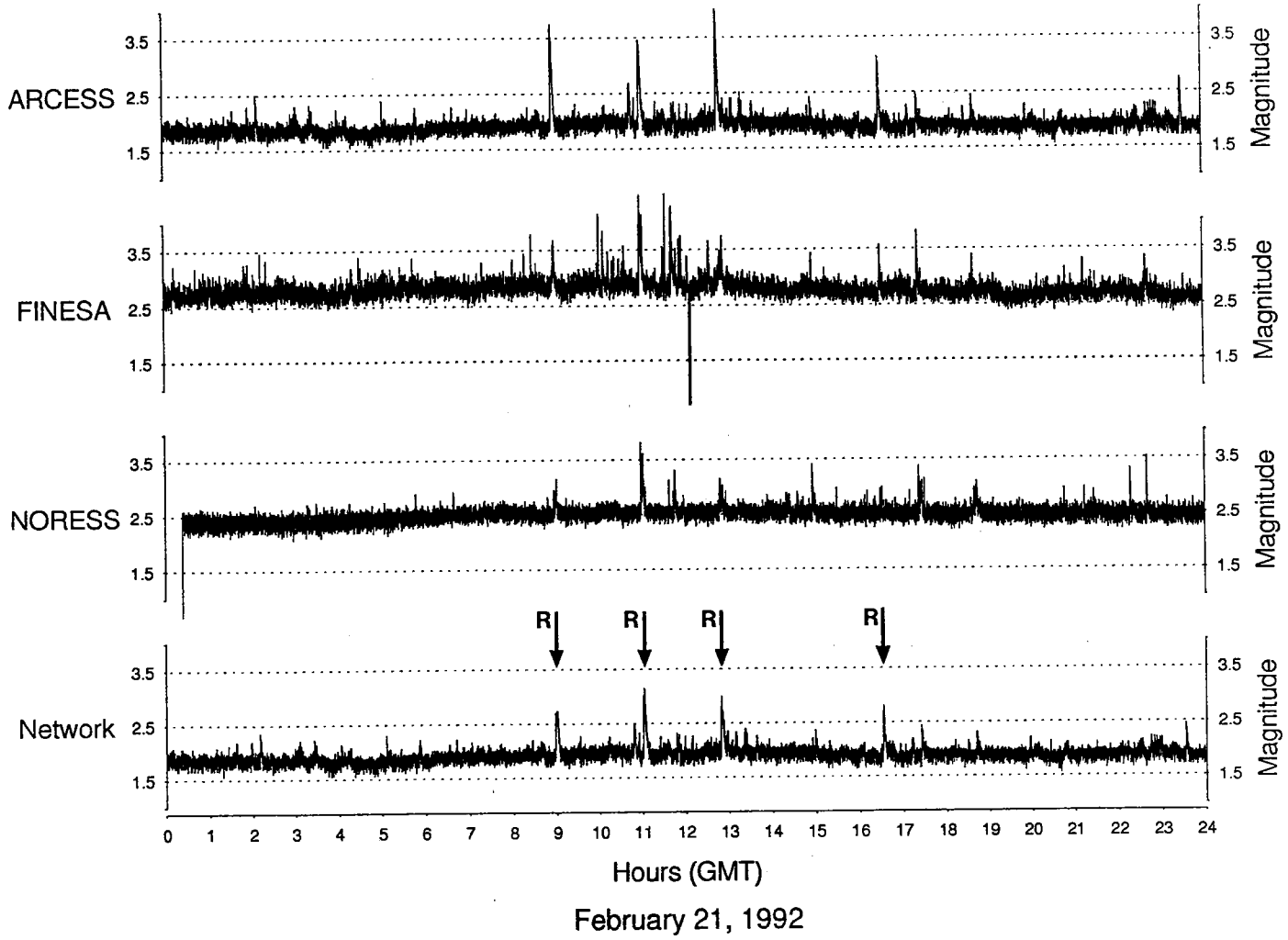

Fig. 7.8.4. The upper three traces represent the 90% magnitude thresholds obtained from the individual arrays, whereas the bottom trace illustrates the network threshold. The arrows indicate peaks with network magnitude threshold exceeding $m_b = 2.6$. A **T** at the arrow indicates that the peak is caused by signals from a teleseismic event, whereas an **R** indicates signals from a local or regional event.

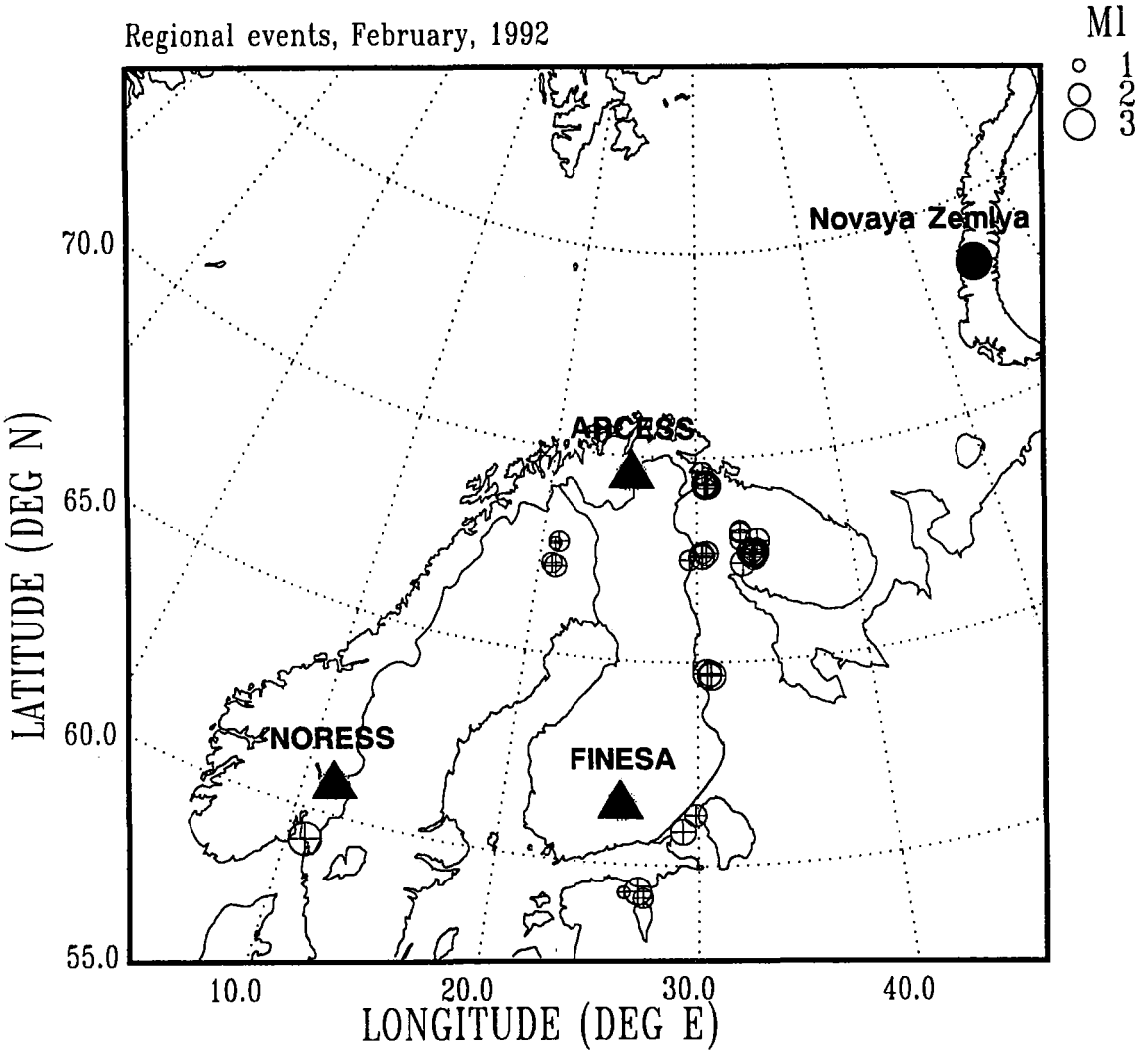

Fig. 7.8.5. Epicenters of regional events causing the network threshold to exceed $m_b = 2.6$. All events, except one felt earthquake in southern Norway, are probable mining explosions. Note the large number of events on the Kola peninsula.

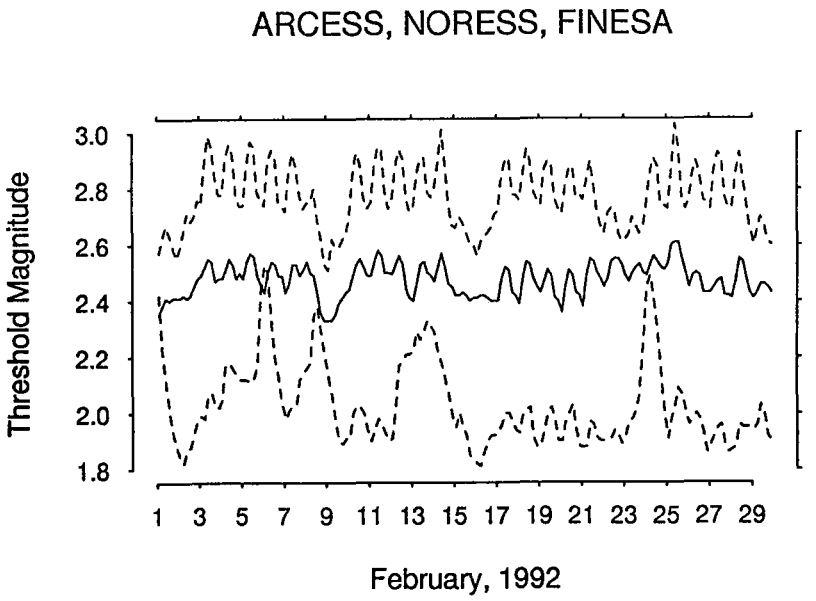

Fig. 7.8.6a. Four-hour medians of the magnitude thresholds for each array for the month of February 1992.

Lower dashed line: ARCESS
Middle solid line: NORESS
Upper dashed line: FINESA

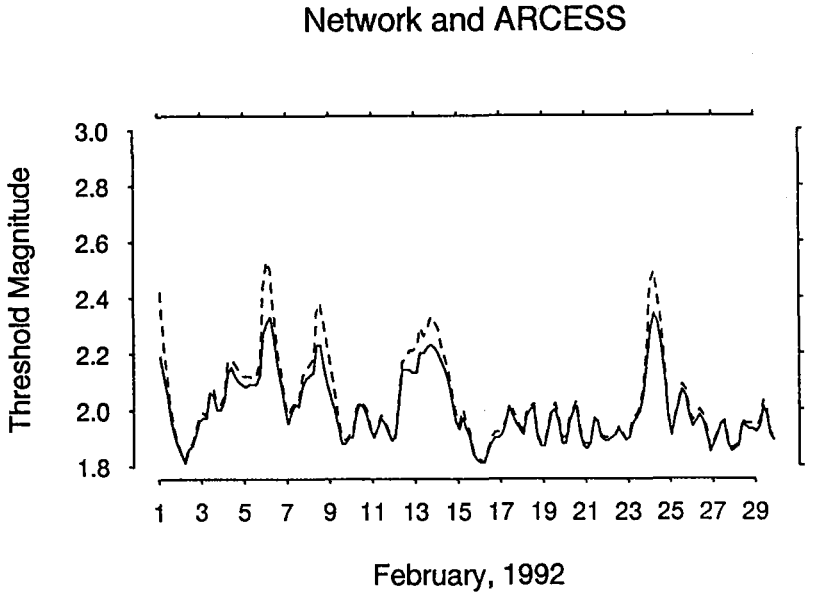

Fig. 7.8.6b. Four-hour medians of the magnitude thresholds for ARCESS and for the network for the month of February 1992.

Solid line: Network
Dashed line: ARCESS

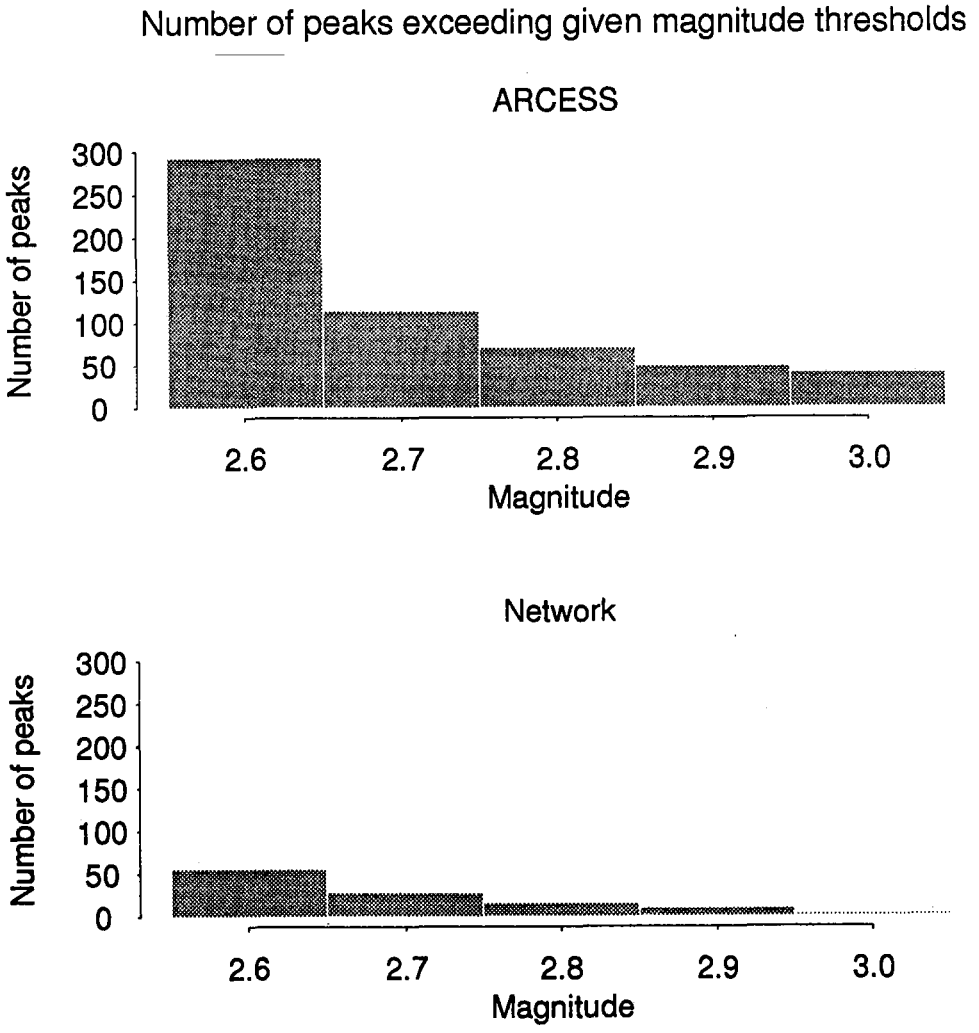

Fig. 7.8.7. Number of peaks exceeding given magnitude thresholds.

Upper part: ARCESS
Lower part: Network